

THE RUTH & TED BRAUN AWARDS FOR WRITING EXCELLENCE  
AT SAGINAW VALLEY STATE UNIVERSITY

# Working Toward a Magneto-Optical Trap

Christopher S. Hopper

COLLEGE OF SCIENCE, ENGINEERING & TECHNOLOGY

*Nominated by Dr. Ming-Tie Huang*

*Assistant Professor of Physics*



Chris Hopper, from Frankenmuth, recently graduated from SVSU with his Bachelor of Science degree, majoring in physics, minoring in mathematics. He is currently attending graduate school at Central Michigan University, where he is also constructing a Magneto-Optical Trap, but now for the study of ultra-cold plasmas. When finished with his M.S. degree at CMU, he plans to transfer elsewhere to obtain a Ph.D. specializing in atomic, molecular, and optical physics.

## Table of Contents

Introduction.....	4
Setting up the ECDL.....	4
Monitoring the Mode Structure .....	6
Finding Resonance.....	7
Resolving the Hyperfine Transitions .....	8
Designing the Ultra-High Vacuum Chamber .....	11
Polarizing the Laser Light.....	13
Future Plans .....	13
Acknowledgements.....	14
Bibliography .....	14

## Table of Figures

Figure 1: Diagram of the External Cavity Diode Laser
Figure 2: Laser Current vs. Power Graph
Figure 3: Mounting of the Diffraction Grating
Figure 4: Spectrum Analyzer Design
Figure 5: 30 mW Spectrum Analyzer Output
Figure 6: 100 mW Spectrum Analyzer Output
Figure 7: Photo of Actual Spectrum Analyzer Constructed
Figure 8: Optical Path Layout for Finding Resonance

Figure 9: Doppler-Broadened Absorption Peaks of $^{85}\text{Rb}$ & $^{87}\text{Rb}$
Figure 10: Graph of <b>Rb</b> Doppler-broadened peaks
Figure 11: Constructed Electronic Components
Figure 12: Difference Amplification of the Absorption Peak of $^{85}\text{Rb}$
Figure 13: FFT Analysis of our Current to Voltage Amplifiers
Figure 14: Absorption Peaks With and Without the Table Being Floated
Figure 15: Measures Taken to Achieve Improved Vibrational Damping
Figure 16: Recessed Mirror of the TEC Diode Housing
Figure 17: Original Vacuum Chamber Design
Figure 18: Actual Vacuum Chamber & Components
Figure 19: 4.5" Optical Mount Design
Figure 20: 2.75" Optical Mount Design
Figure 21: The Zeeman Effect Explained
Figure 22: Optical Arrangement Used to Circularly Polarize the Laser Light
Appendix: The Amplifier Circuit

## Introduction

Magneto-Optical Traps (MOT), devices used for cooling and trapping of neutral atoms, are widely used in atomic physics. One major advantage is that the target atoms can be virtually free of movement from thermal motions because they can be cooled to sub-milli Kelvin temperatures. An MOT traps atoms under vacuum using a total of 7 laser beams of two different frequencies in a quadruple magnetic field. The primary laser, known as the pump laser, is slightly red-detuned to a particular atomic transition frequency. The pump laser is then split into three beams and directed through the vacuum chamber, where these beams are then retro-reflected to produce three pairs of counter-propagating beams. These counter-propagating beams are necessary because they minimize the effect of Doppler-broadening. The secondary laser, known as the re-pump beam, is used to excite the small number of atoms whose electrons populate an energy level that is not able to be excited by the pump laser. Once excited to the desired energy level, these atoms can absorb the photons of the pump beam.

In the presence of an inhomogeneous magnetic field, the atoms will experience what is known as the Zeeman Effect, whereby the atomic transitions will be split into three levels, namely the  $m = 0$  (no magnetic field), or  $\pm 1$ . Because of these two additional transitions levels,  $m = \pm 1$ , the laser beams must be either right- or left-handed circularly polarized. An energy level where  $m = +1$  will absorb the light that is right circularly polarized, where if  $m = -1$ , the atom will absorb the light that is left circularly polarized. The quadruple magnetic field is positioned such that the field strength is zero at the center of the trap and increases as an atom moves away from the center. Thus, with the combination of the laser beams and the magnetic field, one can effectively create the position and velocity dependent forces required for cooling and trapping atoms in an MOT.

## Setting up the External Cavity Diode Laser (ECDL) System

External Cavity Diode Lasers are commonly used in laser cooling and trapping experiments, mainly because they are relatively inexpensive and are fairly easy to tune. Prior to actually setting up the ECDL system, one must either purchase or build the necessary electronics used to monitor the laser output. Our group built the electronics needed. Once this is done, there are three steps involved in setting up the ECDL system, which will be discussed in some detail: collimation of

the diode laser lens, aligning the diffraction grating, and adjusting the laser wavelength.

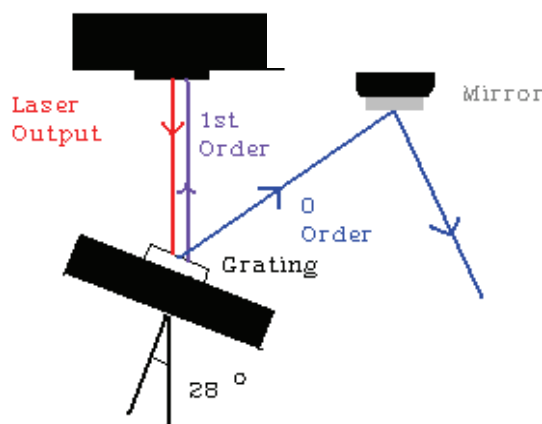
### *Collimation of the Diode Laser Lens*

Diode lasers naturally diverge. For this reason, it is necessary to insert a collimating lens in the system. This lens is placed directly into the laser diode housing. Once the laser diode has been properly placed into the housing with the proper pin configuration, the laser is ready to be powered up. With the laser powered up to a modest current, the lens is then screwed into the laser housing. Using an IR card, one can see how dramatically the laser light is diverging. The goal here is to adjust the lens such that it is exactly its own focal length away from the laser diode. By screwing the lens in and out of the diode housing ever so slightly, the divergence of the laser can be adjusted. The divergence will be minimized when the diameter of the beam is unchanged for a large distance (about four meters or so).

### *Aligning the Diffraction Grating*

By diffracting the laser light so that the first order beam is reflected directly back into the laser diode, one can create an external cavity where the frequency can be controlled (Figure 1).

**Figure 1: Diagram of the External Cavity Diode Laser.** The laser light is diffracted, where the first order light is sent back into the laser diode, while the zero order light is taken out. The grating angle is key in determining the output frequency.

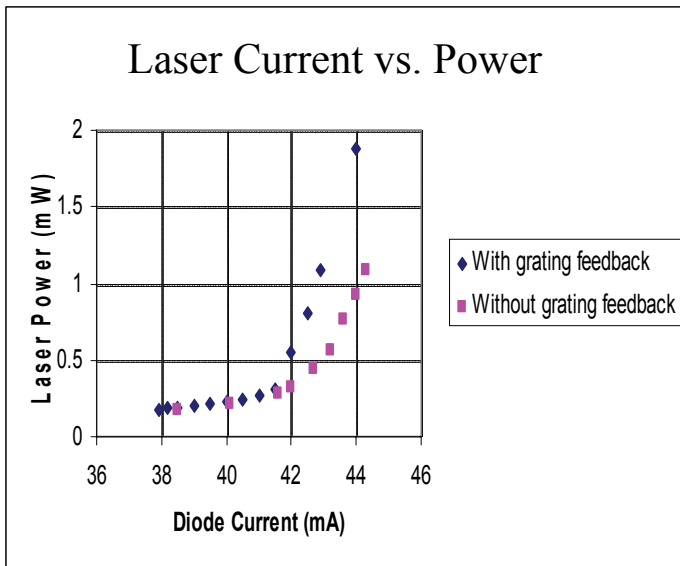


Once the laser has been collimated, the diffraction grating can be attached to a piezo-electric control mounting. Our grating has 1200 lines/mm and has been glued on to an optical blank and screwed into the mounting box (Figure 3).

Before we begin to align the grating, we must determine the actual threshold current for our laser. To

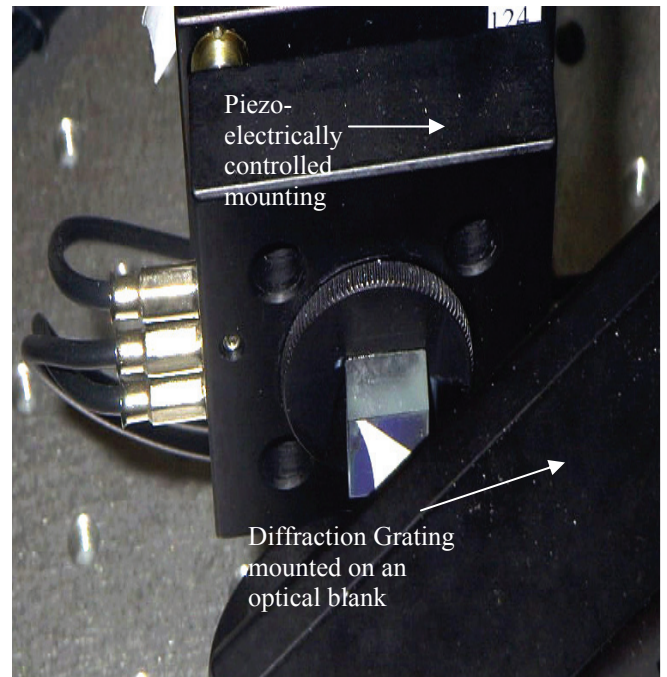
do this, we first refer to the specs of the laser provided by the manufacturer. This gives us an idea of where to begin our search. By using a photodiode to monitor the laser output, we begin at a current just below the threshold shown in the specs of the laser. We can now monitor and record the power at a range of currents. By plotting a graph of current vs. power, with and without grating feedback, we will be able to estimate the threshold current. An example of such a plot can be seen in Figure 2.

**Figure 2: Laser current vs. power graph.** The threshold current is found by determining where the power just begins to increase. This plot is for our 30 mW re-pump laser, and we established that the threshold current was about 39.7 mA.



The angle that the grating makes with respect to the laser is crucial for determining the output wavelength. For the purposes of cooling and trapping rubidium, we would like the wavelength to be approximately 780 nm. Knowing this, the angle of the grating can thus be determined from equation 1:  $2d \sin(\theta_L) = m\lambda$  (1) where  $d$ ,  $m$ , and  $\lambda$  are defined from the grating equation; thus,  $\theta_L = \sin^{-1} [780/(2 \times 833.33)] \approx 28^\circ$

**Figure 3: Mounting of the diffraction grating.**



The piezo-electric mount is equipped with three adjustment screws which are capable of controlling the alignment of the x, y, and z-axes. To approximately align the grating, we need only to affix the grating mount to about  $28^\circ$  from the diode mount, while minimizing the cavity length. Now, the y- and z-axes should be adjusted so that the first order light is reflected back into the diode.

To better align the z-axis, we must use a CCD camera to monitor the beam image as seen on a white index card. When the laser current is set to the threshold level, we can adjust the z-axis knob to look for a brightening in the beam spot. There may be several bright spots throughout the course of adjustment, but to maximize the grating feedback, we can choose the spot with the highest power as read by the laser diode controller.

Once the grating feedback is aligned with respect to the y- and z-axes and the grating is at approximately  $28^\circ$ , we are ready to fine tune the laser wavelength.

### *Adjusting the Laser Wavelength*

As we saw in equation 1, the angle of the diffraction grating is critical to the output wavelength of the laser. This angle can be coarsely adjusted by using the x-axis knob on the grating mount and finely adjusted by applying a scanning voltage to the piezo-electric mount. Using a wavemeter, we can find the initial laser wavelength. We now must turn the x-axis knob either clockwise or counter-clockwise and monitor how the

wavelength changes. We then adjust the wavelength either up or down until we reach the desired value of 780 nm.

### The Electronics

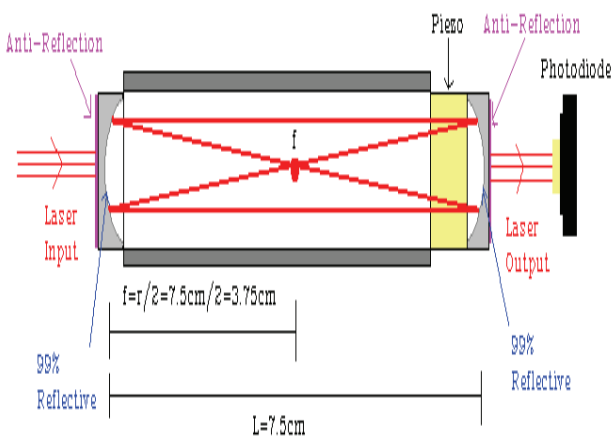
In order to monitor the output of the lasers, we needed to first consider the entire circuit involved (see Appendix). Only a few of the components will be explained in this section; the rest will be described later.

Once we have obtained the desired laser wavelength, we must find the exact resonant transition frequency of rubidium within our vapor cell. To do this we used a photodiode to monitor the laser output power. In order to convert the signal from the photodiode to one that we can read with an oscilloscope, we had to construct several electronic components (Figure 11). First, we needed a 15-12 volt amplifier to power the photodiodes. Then we needed two current-to-voltage amplifiers to convert the signal. These amplifiers have an adjustable gain knob so as to not saturate the photodiodes. Once the laser signal has been converted, we can read the output on the oscilloscope.

### Monitoring the Mode Structure

While trying to achieve the desired atomic transitions, it is essential that the lasers are operating in single mode. To determine the mode structure of the lasers, we constructed a spectrum analyzer. The design of the spectrum analyzer can be seen in Figure 4; the actual analyzer is pictured in Figure 7.

**Figure 4: Spectrum Analyzer design.**



Our spectrum analyzer consists of an aluminum tube with one mirror fixed to each end. One mirror is glued to a piezo disk, which is glued to the analyzer itself. The laser beam enters the analyzer at one end while a scanning voltage is supplied to the piezo disk, causing it to expand and contract. This variation in the piezo disk causes the cavity length to change. When the cavity length is such that a standing wave is created within the analyzer, the laser light is able to exit and be detected by a photodiode. If the laser is multi-mode, light will exit the analyzer at several points during the expansion and contraction of the piezo. In contrast, when the laser is operating at single mode, the light is able to escape only at one particular cavity length. We found that both the 30 mW re-pump and the 100 mW pump laser are indeed single mode (Figures 5 & 6).

**Figure 5: 30mW Spectrum analyzer output.** This is the single mode output of the 30 mW re-pump laser.

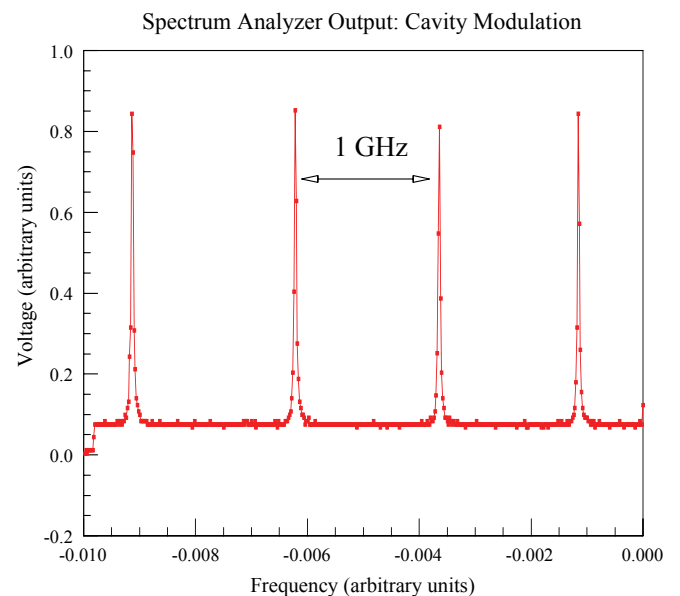


**Figure 6: 100 mW Spectrum analyzer output.** This is the single mode output of the 100 mW pump laser.

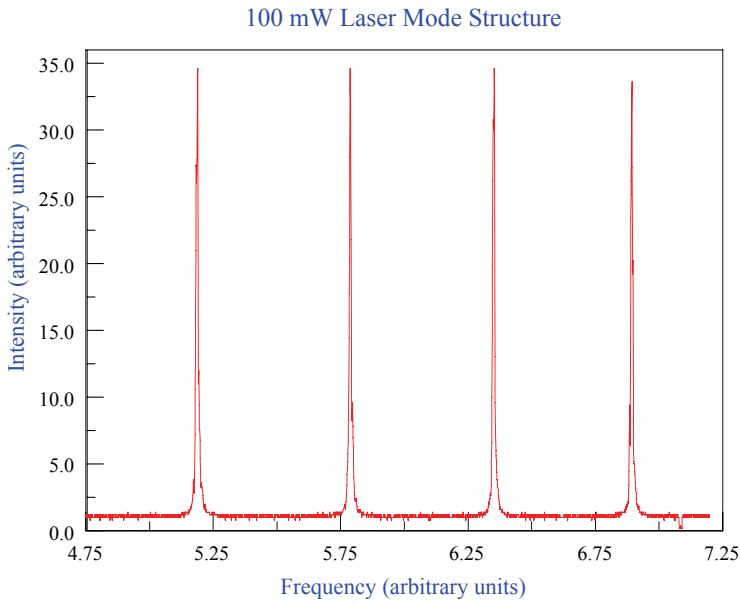
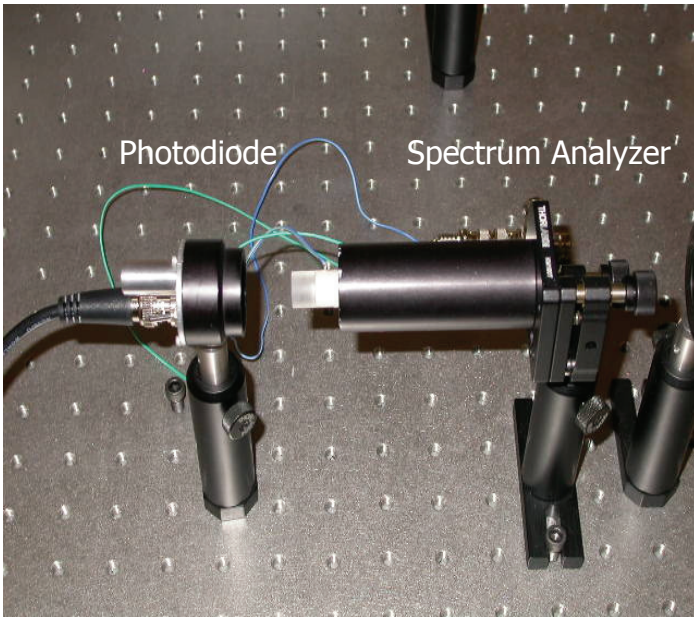


**Figure 7: Photo of actual spectrum analyzer constructed.**

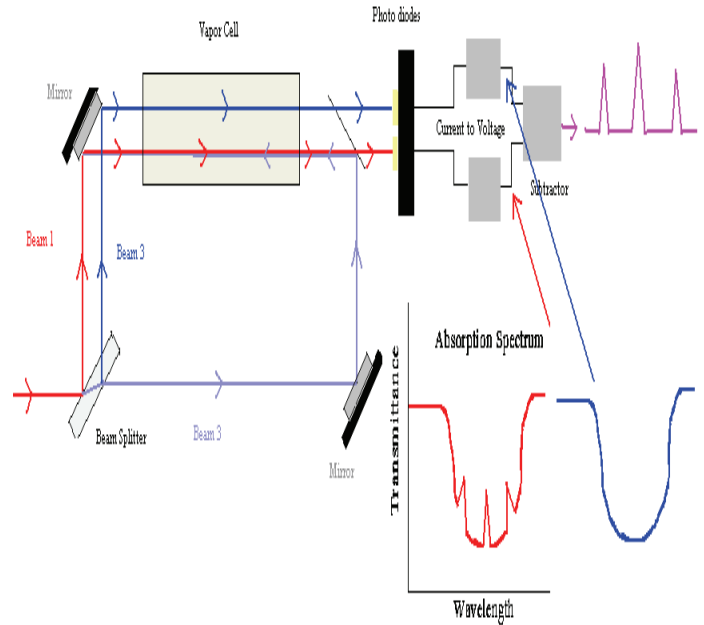


## Finding Resonance

Once the laser frequency and mode structure have been determined to be at the desired values, it is time to find resonance within the vapor cell. To do this, we need to shine the laser light through the vapor cell in the configuration shown in Figure 8, supply a scanning voltage to the piezo-electric grating mount, and monitor

the laser output with a photodiode and numerous electronic components.

**Figure 8: Optical path layout for finding resonance with the ECDL.**

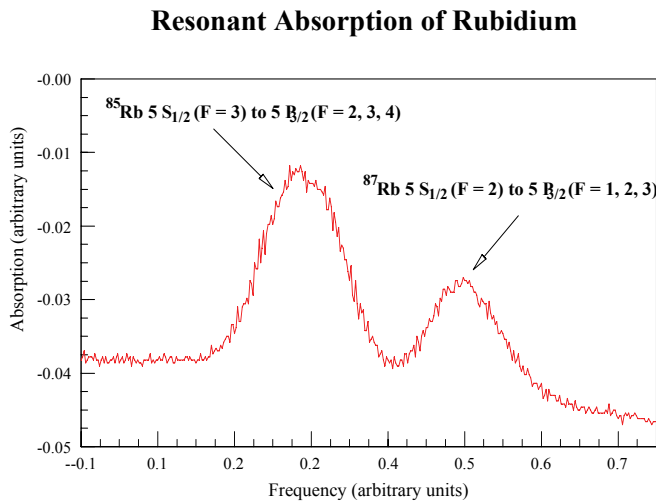


### Optical Path Layout

To simply find resonance, one only needs to shine one beam through the Rb cell while scanning the grating angle and monitoring the laser power output. However, in order to see individual hyperfine transitions, we need a much more complicated set-up. With only one beam passing through the cell, we see all of the hyperfine transitions “smeared” together, which is known as Doppler-broadening. This broadening occurs because of the different velocities with which the atoms are moving with respect to the lab reference frame. The velocities of atoms can be categorized into three basic classes: those moving toward the laser, those moving away from the laser, and those moving perpendicular to the laser. These three classes all contribute to the Doppler-broadened peak. Atoms moving toward the laser see the frequency blue-shifted and contribute to the lower frequency side of the Doppler profile. Those moving away from the laser see the light red-shifted and contribute to the higher side of the Doppler profile. Atoms moving perpendicularly with respect to the laser beam contribute to the peak of the profile and see the light at the lab view frequency.

While scanning the grating angle with a voltage of about 60 V and at a frequency of about 0.5 Hz, we can observe the Doppler-broadened peaks of the two isotopes of rubidium in the vapor cell, namely  $^{85}\text{Rb}$  and  $^{87}\text{Rb}$ , which are seen in Figure 9.

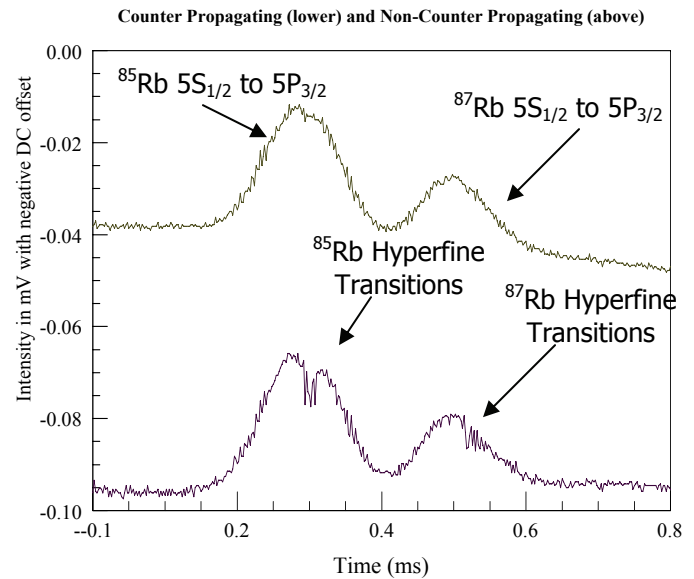
**Figure 9: Doppler-Broadened peaks of rubidium.**  $^{85}\text{Rb}$  is more abundant than  $^{87}\text{Rb}$ , hence the higher absorption peak.



In order to see individual hyperfine transitions, we must minimize the effect of Doppler-broadening. To do this, we must employ the beam used to find the broadened peaks along with a counter-propagating beam and the electronic components we built. The beam path seen in Figure 9 was used for this purpose.

First, we must split the original beam with a beam splitter to obtain three beams. Two of the beams (known as the probe beams) are sent through the vapor cell from the same direction. The third beam (the pump beam), which is much stronger than the probe beams, is sent back through the vapor cell such that it counter-propagates with one of the probe beams. Now, these two beams are competing for the same atoms, which have zero velocity with respect to the lasers; they are traveling perpendicularly to the beams. In this case, absorption of the probe beam will be reduced at one particular point in the scanning range. More specifically, during the scanning, we see the familiar Doppler-broadened profile with the addition of an increase in probe beam intensity at a particular point which corresponds to the point at which the beams are competing for the zero velocity atoms. Since the pump beam is more intense, it has a higher probability of interacting with these atoms. Once these atoms are excited by the pump beam, they cannot be excited by the probe beam until they decay, which means that they are removed from the pool of atoms that can be excited by the probe beam. The final result is that we see the Doppler-broadened peaks with small Lamb dips in them. These Lamb dips represent the individual hyperfine transitions, which can be seen in Figure 10.

**Figure 10: Graph of Rb Doppler-broadened peaks.** The lower graph shows the Lamb dips which represent the individual hyperfine transitions.

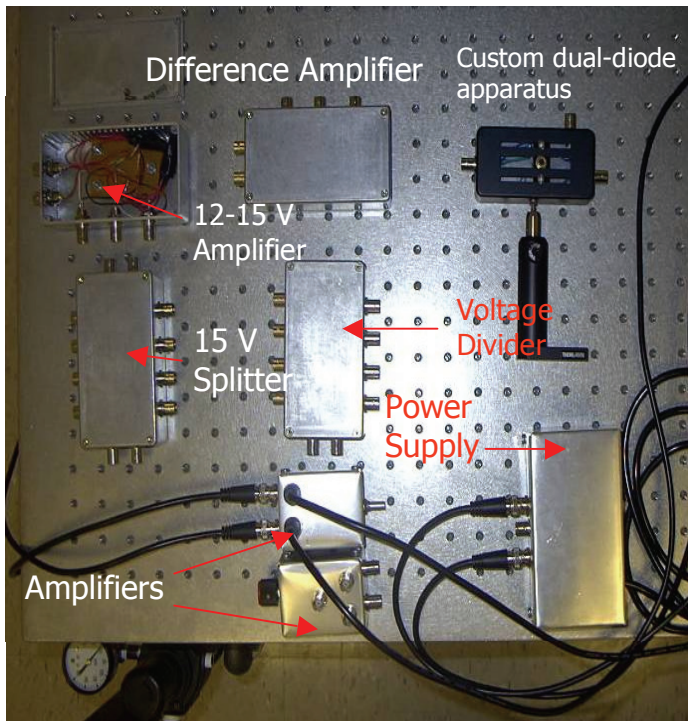


In order to pinpoint these individual hyperfine transitions, we must employ more of the electrical components that we built.

## Resolving the Hyperfine Transitions

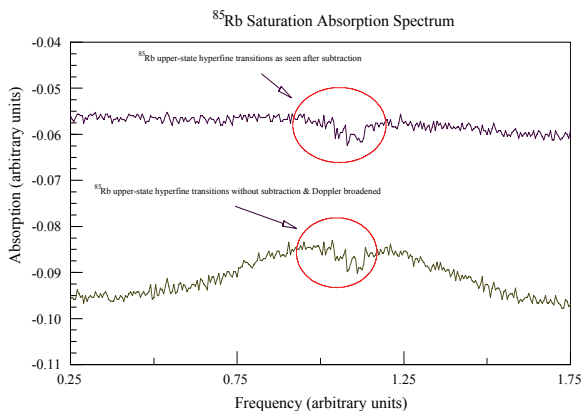
Resolving these individual hyperfine transitions is not a difficult task, once we have laid out the optical path shown in Figure 8 and constructed the proper electronic components. With reference to Figure 8 and the complete circuit shown in the Appendix, we see that we need to have three beams passing through the vapor cell: a probe beam on its own, plus a probe beam with a third counter-propagating pump beam. These three beams are thus converged into two beams, which can be detected by a custom dual-diode apparatus. This apparatus, which needs a 15 V-12 V amplifier since it is powered by only 12 V, has the counter-propagating beam subtracted from the non-counter-propagating beam. In order to accomplish this, we use a difference amplifier, which we built (components seen in Figure 11).

**Figure 11: Electronic components that we built.**



One of the beams detected by the dual-diode apparatus is strictly Doppler-broadened. The other beam, which has a counter-propagating element, has the familiar Lamb dips seen in Figure 10. When these two beams are subtracted from each other with a difference amplifier, we are left with only the individual hyperfine transitions, seen in Figure 12.

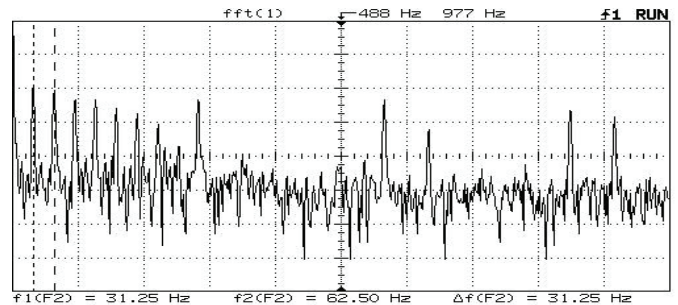
**Figure 12: Hyperfine transitions of  $^{85}\text{Rb}$  revealed by difference amplification of the counter propagating and non-counter propagating beams after being sent through the Rb vapor cell.**



### The Problem of Noise

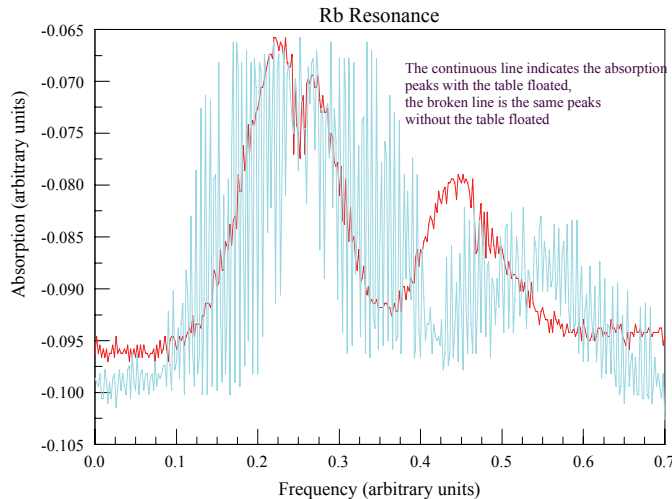
It is clear from Figure 12 that we encountered a noise problem in our optical system. This is apparent because, clearly, the non-subtracted and subtracted signals are not significantly different enough to actually identify individual hyperfine transitions. In order to eliminate this noise, we first had to identify its source. The easiest noise to eliminate would be that introduced by the electrical components we built. To determine if this was in fact the source, we examined the signals produced by these different components with the FFT function of a digital oscilloscope. The results can be seen in Figure 13. Clearly, there is an electrical component of noise introduced by the current-to-voltage amplifiers; however, this noise is not random, but rather is produced in intervals of approximately 30 Hz.

**Figure 13: The FFT signal from our current-to-voltage amplifiers. The period is approximately 30 Hz, which is clearly not random like we see in Figure 12.**



Now that it had been determined that the random noise was not caused by our electrical components, we looked elsewhere. Our lab is located on the second floor, near a first floor mechanical room. In light of this fact, we wanted to see what our absorption spectrum would look like when the optical table was not being floated. This experiment shed a great deal of light on the source of our noise problem. Figure 14 shows the absorption spectrum without the table being floated.

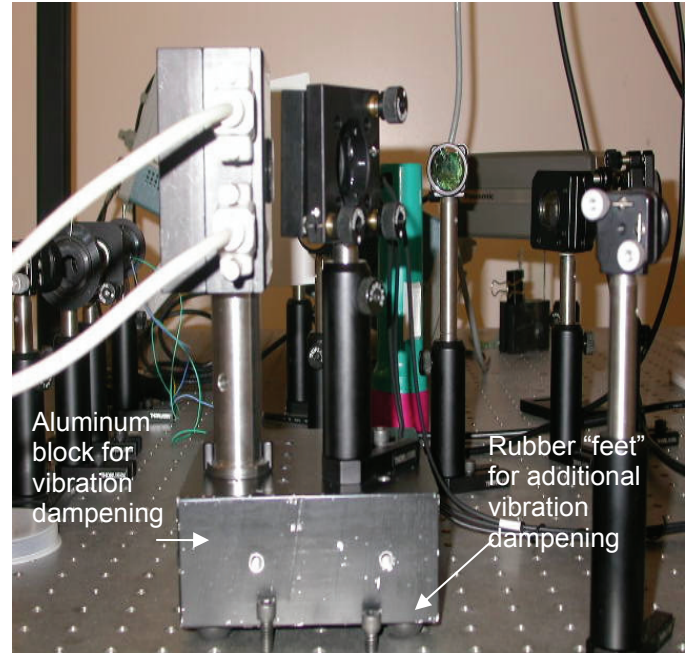
**Figure 14:** To identify the source of noise, we looked at the absorption peaks with and without the optical table being floated. The narrow continuous line indicates the peaks with the table floated, and the broad broken line is without the table being floated. Clearly, there is a strong source of mechanical vibrational noise.



From Figure 14 it is clear that the source of our noise was indeed from mechanical (and possibly acoustic) vibrations in the second floor lab. This problem needed to be addressed in order to fully resolve the hyperfine transition frequency which we wished to lock our laser to.

The first step taken was to introduce a damping material between our ECDL and the optical table. Figure 15 shows the thick aluminum block and rubber "feet" placed on the bottom of the block that we set the diode laser on, in order to achieve this. This block serves an additional purpose. That is, it has allowed us the portability needed to test our ECDL in another lab, in hopes of finding the desired individual hyperfine transition frequencies.

**Figure 15:** The ECDL set up on a thick aluminum block with additional damping "feet" that the block sits on.

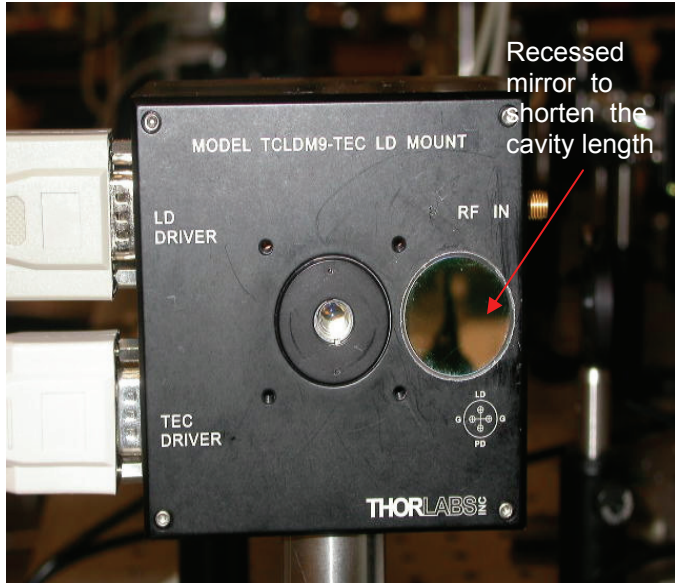


These improvements did provide a modest level of additional vibration dampening; though it was still not enough for our purposes, the system was now able to easily be transported to another lab for testing.

We now took our ECDL, optics, electronics, and Rb vapor cell to a downstairs lab. The same optical system was set up and tested. Unfortunately, we did not have good results. Resonance was not found during the period of time in which we had access to the lab. Once we were again set up in our original lab, we determined that the reason for our inconclusive results was that the 30 mW diode we were using was no longer operating in single mode. This caused us to be unable to stabilize the laser enough to attain the 780 nm wavelength necessary to achieve resonance.

Another measure taken in order to reduce the effect of mechanical and acoustic vibrations on our laser was to shorten the external cavity length. Originally, the mirror used to redirect the zero order light (see Figure 1) was glued directly to the surface of the diode laser housing. In this set-up, the only way to shorten the cavity length is to recess the mirror into the mount, thus allowing the cavity to become shorter, while increasing the angle of the outgoing zero order light. The recessed mirror can be seen in Figure 16.

**Figure 16: The TEC Laser Diode mount with the zero order reflection mirror recessed into the face plate in order to reduce the EC length.**

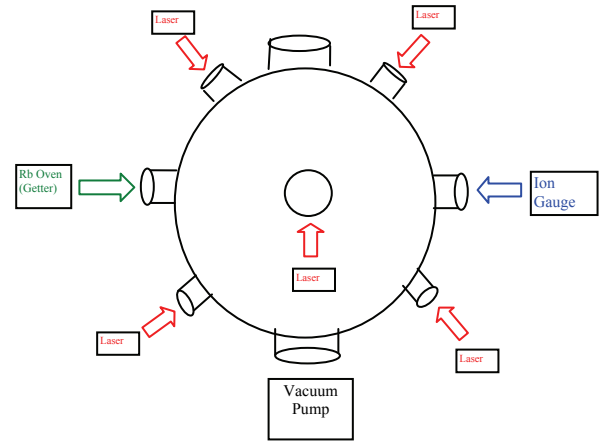


In addition to these measures taken, we also designed a sound dampening enclosure to house our ECDL systems. While making these improvements to our hyperfine transition resolution, we continued to move forward in other areas of our project.

## Designing the Ultra-High Vacuum Chamber

The two most important considerations taken in the initial phases of designing the vacuum chamber were geometry and number of the ports. The first phase of our experiments involved testing the parameters of the MOT. To do this, it was determined that we would initially need 10 ports: 6 for the lasers, one for the Rb getters, one for the CCD camera, one for the TC gauge, and one for the Turbo-Molecular vacuum pump. The most important component of the chamber geometry is that the three pairs of windows for the lasers all be orthogonal to each other, thus covering the x- y- and z- axes. This requirement was easily satisfied with a spherical chamber. The original design can be seen in Figure 17.

**Figure 17: Vacuum Chamber & Rb Oven Design**



The only requirement for the other four ports is that they must be directed toward the center of the chamber. The chamber we purchased is an 18" spherical chamber with a total of 20 ports.

The next task was to determine the number and size of the windows we would need. Of course, six windows are needed for the lasers, with one additional window for the CCD camera. For the laser windows, one further consideration must be made, namely the anti-reflection coating. The coating on our windows has a transmission of  $>99.5\%$  for light of wavelength 780 nm.

To inject the Rb into the chamber, the Getters needed a current source, provided to them through a special feed-through flange that allowed us to heat and therefore discharge the Rb atoms from up to three Getters. This flange was also purchased.

We estimated that the chamber, when equipped with all of the flanges, windows, gauges, blanks, and optics, would weigh over 150 lbs. Therefore we also needed to design and build a sturdy support frame that would allow us complete, unhindered access to all 20 ports. A member of our group designed this support frame, and the SVSU maintenance department constructed it for us.

To achieve and maintain the vacuum pressure we needed (at least  $1 \times 10^{-7}$  Torr), we also had to acquire a Turbo-Molecular Vacuum Pump. We found a used model for a reasonable price, which, with a special adapter flange, could be connected to the roughing pump we already had.

**Figure 18: The vacuum chamber and support frame of the SVSU Atomic Physics Lab.**

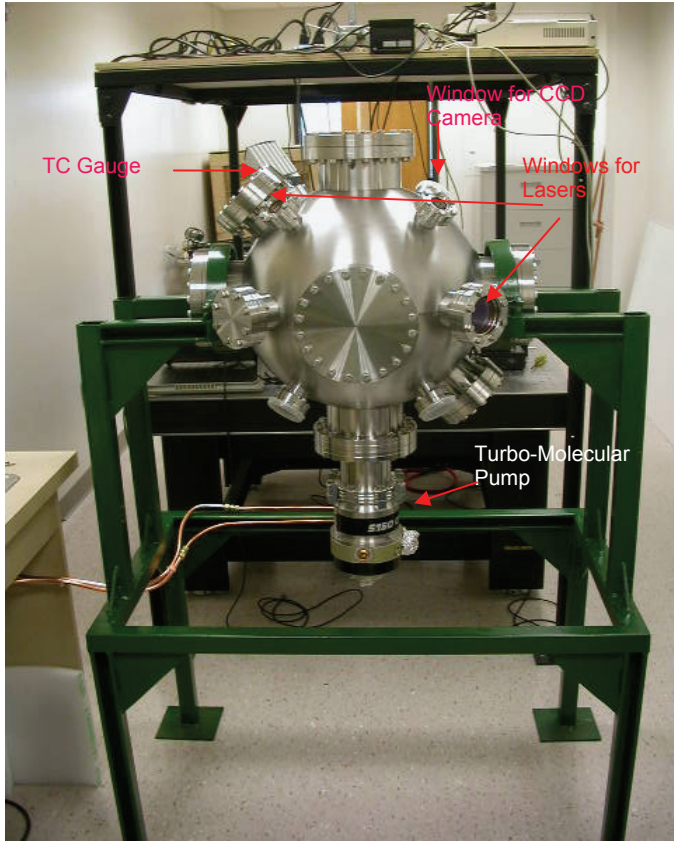


**Figure 19: Optical mount design for the 4.5" windows.**

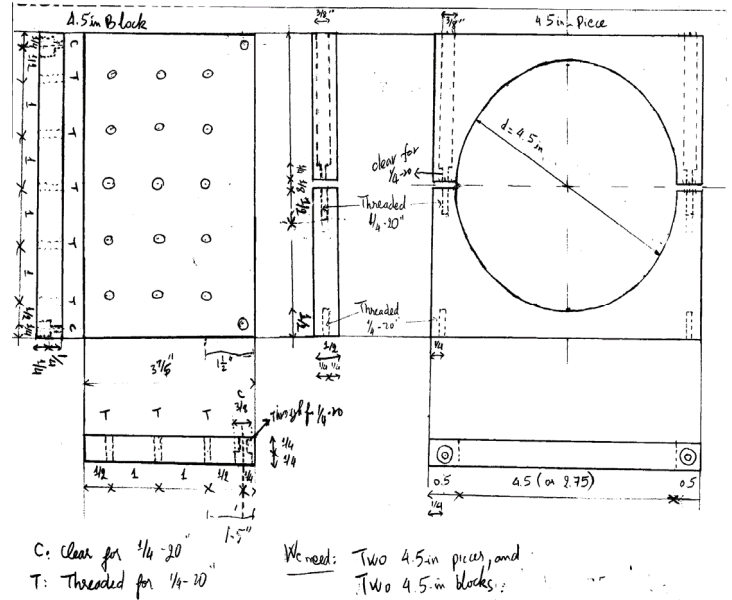
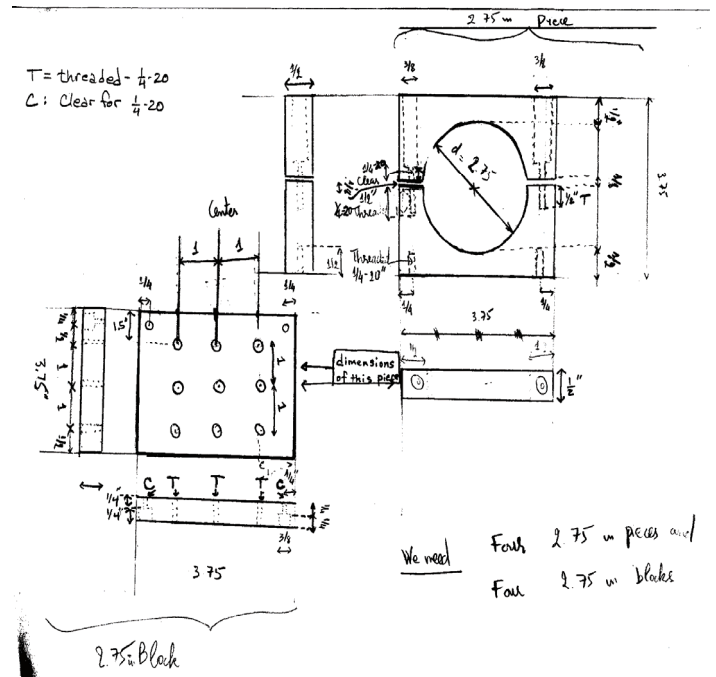


**Figure 20: Optical mount design for the 2.75" windows.**



*Optics for the Chamber*

In order to produce the necessary counter propagating, circularly polarized laser light, our pump beam needed to be split into three equal intensity beams. To accomplish this, we purchased a 1/3-2/3 and a 50/50 beam splitter. The original light would be split into one beam with 1/3 the intensity and a second beam with 2/3 the intensity. This second beam would then be divided into two beams of equal intensity. All three beams then needed to be directed to the windows on the chamber. To catch the beams at the windows, we needed to design and construct special optical mounts. These mounts allowed us to attach mirrors and  $\lambda/4$  waveplates to six of the windows. One additional mount had to be fabricated to hold the CCD camera. Schematic diagrams of the optical mounts can be seen in Figures 19 and 20. The idea is that a thin square aluminum plate with a hole bored in the center (of the same diameter as the port it is to be attached to) can be cut into two halves. These halves can then be secured together around the respective window. Once this is done, a small breadboard can be attached to the bottom, which will hold the mirror and waveplate.

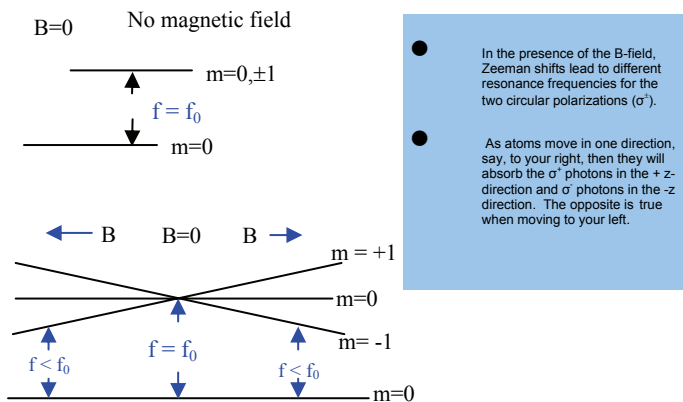
## Polarizing the Laser Light

In the presence of a magnetic,  $\mathbf{B}$ , field, the atomic energy transitions will shift. The energy levels will take the quantum number of  $\Delta m = 0$  or  $\pm 1$ . This is known as the Zeeman Effect (see Figure 21).

As the atoms move further away from the center of the trap (where  $\mathbf{B} = 0$ ), they will see the red-detuned laser light at the correct frequency for absorption. In one direction,  $\Delta m = -1$  (corresponding to left-circularly polarized light) and the other direction,  $\Delta m = +1$  (corresponding to right-circularly polarized light).

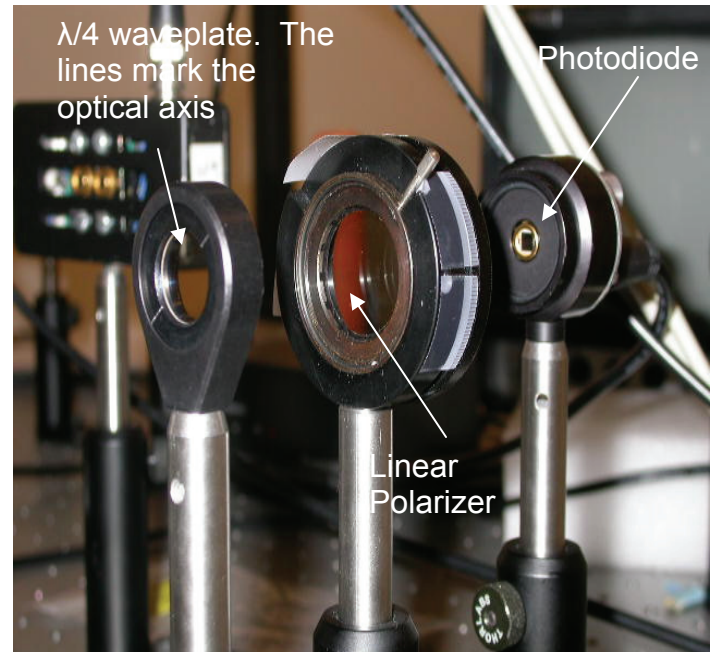
Our lasers are naturally vertically polarized. To perform the correct circular polarization, we employed two  $\lambda/4$  waveplates on either side of the three counter-propagating beams passing through the MOT. This polarization, along with the magnetic field, gave us the position-dependent force we needed to trap the atoms.

**Figure 21: Explanation of the effect that a magnetic field has on the frequency of atomic transitions, known as the Zeeman Effect.**



In order to circularly polarize our lasers, we passed them through a  $\lambda/4$  waveplate. The waveplate must lie in a plane exactly perpendicular to the incident beam, and be rotated  $45^\circ$  from the vertical. To ensure that the laser light was indeed circularly polarized, we measured the power of the beam without any obstructions. We then inserted the  $\lambda/4$  waveplate and the linear polarizer. When the angle of the waveplate was correct, there would be no change in power as we rotated the linear polarizer.

**Figure 22: Optical arrangement used to circularly polarize the laser light. When the optical axis of the  $\lambda/4$  waveplate is at  $45^\circ$ , the intensity of the laser (measured with the photodiode) will not change for any rotation of the linear polarizer.**



## Future Plans

In the immediate future, we need to do several things. First, we have to pump down the chamber to see if we are able to achieve the necessary vacuum pressure. This will be done in the very near future. Secondly, we will set up the chamber optics (when the mounts are completed) and direct the three beams through the chamber. We will then be ready to dispense Rb into the chamber and find resonance. Once our noise problems are corrected, we will be able to lock the lasers to a precise hyperfine transition (with our lock-in amplifier). Once all of this is complete, we will design and construct the anti-Helmholtz coils to provide us with the magnetic field. We will then be able to proceed in trapping Rb atoms. After atoms have been successfully trapped, we will measure the efficiencies and parameters of the MOT.

## Bibliography

- Chen, C. Y., Y. M. Li, K. Bailey, T. P. O'Connor, L. Young, & Z.-T. Lu. 1999. Ultrasensitive isotope trace analyses with a magneto-optical trap. *Science* 286: 1139.
- Du, X., K. Bailey, Z.-T. Lu, P. Mueller, T. P. O'Connor, & L. Young. 2004. An atom trap system for practical  $^{81}\text{Kr}$ -dating. *Review of Scientific Instruments* 75: 3224.
- Metcalf, H. J., & Straten, P. 1999. *Laser Cooling and Trapping*. New York: Springer-Verlag.
- Moore, I. D., K. Bailey, J. Greene, Z.-T. Lu, P. Mueller, T.P. O'Connor, Ch. Geppert, K.D.A. Wendt, & L. Young. 2004. Counting individual  $^{41}\text{Ca}$  atoms with a magneto-optical trap. *Physical Review Letters* 92: 15302.

## Acknowledgements

- Dr. Frank Chen for the use of many optical components and his lab space.
- The SVSU maintenance department for building our vacuum chamber support frame and hooking up the water cooling lines to our TM pump.
- Mr. John Leonard for constructing many of our custom mounts.
- Dr. Jonathan Leonard for helping me rule out electronic noise as a problem in our circuit.

## Appendix

### The amplifier circuit

Figure 4 - Amplifier Circuit

